Analysis of Creep Curve of Reinforced Concrete Beams with Eurocode 2 via the Three-Parameter Model

Mateus M. Barretto[1], Alexandre M. Wahrhaftig[1,2]

[1,2]*Graduate Program in Civil and Environmental Engineering (PPGECEA), State University of Feira de Santana (UEFS)*
Avenida Transnordestina, s/n - Novo Horizonte, 44036-900, Feira de Santana/Bahia, Brasil
eng.mbarretto@hotmail.com
[2]*Department of Construction and Structures (DCE), Federal University of Bahia (UFBA)*
Rua Aristides Novís, 02, 5º andar, Federação, 40210-630, Salvador/Bahia, Brasil
alixa@ufba.br

Abstract. This study seeks to analyze the use of the rheological model of Three-Parameter to represent the effects of creep in reinforced concrete structures. An empirical adjustment is done to approximate the obtained curve to that existing in Eurocode. The deformation of two beam models is assessed using the following mathematical paths: firstly, the European Standard EN 1992-1-1 2023 is used. Next, the three-parameter viscoelastic model is searched to do its curve to match that of Eurocode admitting a difference averaged of results previously established. A basic literature review on creep in concrete structures is presented, followed by a structural analysis for an expected lifetime. Deflection curves were generated by using numerical simulations. With that, it was possible to assess comparatively the displacements of the beams axis over time, considering the creep for both the Eurocode and Rheological Model assuming an average difference of results less than 5% over 41 years.

Keywords: creep, three-parameter model, concrete beams, deformation, eurocode2

1 Introduction

Excessive deformations in reinforced concrete structures affect the architectural aesthetics of the construction, reduce the durability, and compromise the safety of the structures. This phenomenon is directly associated with concrete creep, which occurs when structures are subjected to loads over an extended period according to Tran [1]. Concrete creep significantly influences the long-term performance of structures components made of this material (Giorla [2]; Liang and Wei [3]).

Creep can be defined as the increase in deformation under constant stress over time. This phenomenon has a critical effect on the service limit state of reinforced concrete structures because it leads to an increase in the deformations of beams and slabs, promoting the redistribution of stresses between the concrete and the reinforcement (Goel [4]; Shao *et al* [5]). In reinforced concrete beams, creep strains reduce the stresses in the concrete mass and increase the stresses in the reinforcement bars, potentially inducing them to yield, as stated by Madureira *et al*., [6] and Wahrhaftig *et al.,* [7].

Long-term behavior creep depends on various parameters, such as the age of the concrete at the time of load application, curing conditions, environmental conditions such as relative humidity, the level of applied stress, the duration and history of loading, the dimensions of the concrete elements, and the material composition (Hassoun and Manaseer [8]; Hubler *et al*., [9]; Magalhães *et al*., [10]). Other factors that favor the occurrence of creep include the water-cement ratio, stress/strength ratio, temperature, and water content in the cement paste at the time of load application (Neville and Brooks [11]; Paulson *et al*., [12]).

According to Wahrhaftig [13], creep is associated with the rheological behavior due to the viscoelastic nature of certain materials, resulting in a continuous increase of deformations even under constant stress. In this context, rheological models used to represent the viscoelastic behavior of many solids are usually based on the association of springs and dashpots that predict the total strain and aim to describe more accurately the behavior of each material or group of materials. In this study, the generalized Kelvin-Voigt model with three parameters is utilized to compare the final deflection of a simply supported and a cantilevered-free reinforced concrete beams. For doing that, it was necessary to use the parallel axis theorem and the section homogenization theory.

2 Creep Criterion According to Eurocode

According to Eurocode 2 (2023), EN 1992-1-1 [14], the phenomenon of concrete creep depends on environmental humidity, the dimensions of the structural element, the composition of the concrete, the age of the concrete at the time of initial loading, as well as the duration and intensity of the applied loads. In situations where it is necessary to calculate the creep coefficient as a function of time, the Annex B.1 must be observed. This regulation provides the expressions for determining the creep coefficient as a function of time. In this case, the creep coefficient, $\varphi(t)$, is obtained by:

$$\varphi(t) = \varphi_{bc}(t) + \varphi_{dc}(t) \tag{1}$$

where:

ϕ_{bc} is the basic creep coefficient.

ϕ_{dc} is the drying creep coefficient.

EN 1992-1-1 indicates all steps to reach eq. (1). According to Eurocode 2 (2023), the effect of creep should be considered through the effective modulus of deformation, as per eq. (2).

$$E(t) = \frac{1.05Ecm}{1 + \varphi(t)} \tag{2}$$

where Ecm is the modulus of elasticity of concrete calculated for 28 days after its production.

3 Rheological Model for Representing the Creep

Viscoelastic behavior is time-dependent. This means that viscoelastic materials, when subjected to constant stress, produce strains that increase over time, or when subjected to constant deformation, result in decreasing stresses over time (Carvalho [15]). The Kelvin-Voigt model can be represented by the parallel association of an elastic element and a viscous element (Marques and Creus [16]). Being a parallel association, it is understood that both basic models will be subjected to the same deformation and that the sum of the stresses in each model equals the total stress σ. The parameter E determines the tendency for total deformation and represents the modulus of elasticity of the material in elastic behavior. Additionally, the parameter η represents the viscosity modulus of the material, which determines the rate of deformation over time and provides a viscoelastic behavior to the material.

According to Wahrhaftig *et al.,* [17] one model used to represent the viscoelasticity of solids is the three-parameter model, in which the elastic parameter E_0 is connected to the viscoelastic Kelvin-Voigt model with parameters E_1 and η_1, which is a simplification of the Group I Burgers model, as shown in Fig. 1.

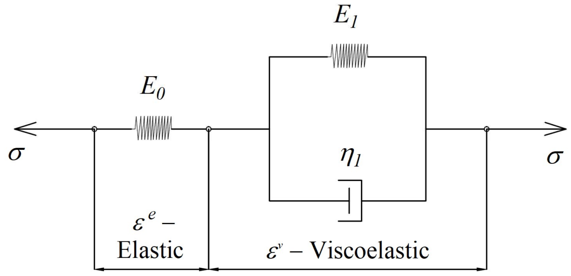

Figure 1. Generalized Kelvin-Voigt model with three parameters

The total strain of the model of three parameters is given by $\varepsilon = \varepsilon^e + \varepsilon^v$, where is the strain of the elastic model, and is the strain of the Kelvin-Voigt model. When differentiated with respect to time, the total strain is obtained as

$$\dot{\varepsilon}(t) = \dot{\varepsilon}^e(t) + \dot{\varepsilon}^v(t) \tag{3}$$

which is the constitutive equation of the elastic and Kelvin-Voigt models, respectively. Considering $E_1 = E_0$ as the modulus of elasticity for both parts of the rheological model,

$$\sigma(t) = E_0\varepsilon^e(t) \quad \text{and} \quad \dot{\sigma}(t) + \frac{E_0+E_0}{\eta_1}\sigma(t) = E_0\dot{\varepsilon}(t) + \frac{E_0E_0}{\eta_1}\varepsilon(t) \tag{4}$$

are found. From the previous equations, one derives the following differential equation:

$$\sigma(t) = E_0\varepsilon^v(t) + \eta_1\dot{\varepsilon}^v(t) \tag{5}$$

where $\sigma = 0$ for $t < 0$ and $\sigma = \sigma_0$ for $t > 0$, with t representing the time and $t = 0$ the instant of loading application. As the stress remains constant, the stress derivative with respect to time is zero. Applying the previous stress condition, the following ordinary differential equation is found:

$$E_0\dot{\varepsilon}(t) + \frac{E_0E_0}{\eta_1}\varepsilon(t) = \sigma_0(t) \tag{6}$$

for which the general solution for $t > 0$, taking the initial condition $\varepsilon(0) = \sigma_0/E_0$, is

$$\varepsilon(t) = \sigma_0\left[\frac{1}{E_0} + \frac{1}{E_0}\left(1 - e^{-\frac{E_0}{\eta_1}t}\right)\right] \tag{7}$$

Obviously, if the stress level remains constant, the modulus of elasticity should decrease concurrently with increasing strain. Therefore:

$$E(t) = \frac{1}{\frac{1}{E_0} + \frac{1}{E_0}\left(1 - e^{\frac{E_0}{\eta_1}t}\right)} \tag{8}$$

Equation (8) can be written to explicitly a creep coefficient:

$$E(t) = \frac{E_0}{1 + \varphi(t)} \tag{9}$$

with

$$\varphi(t) = \frac{\left(1 - e^{\frac{E_0}{\eta_1}t}\right)}{\propto} \tag{10}$$

where α serves as a regulator for the amplitude of the curve.

4 Numerical simulation

Two models are adopted: a simply supported beam and a cantilevered beam, Fig. 2, (a) and (b), respectively. For both models, the geometric linear analysis is characterized by the approximate equation of the elastic line, and by the modulus of elasticity as a function of time. The numerical simulation was performed using Mathcad software. The properties of reinforcement steel and concrete are considered by using the theory of homogenized section. The temporal modulus of elasticity, $E(t)$, indicated in eqs. (9) and (10), assumes the form established in eqs. (2) and (8).

To define the viscous parameter of the rheologic model, an empirical adjustment using eqs. (1) and (10) was performed to obtain an average of difference of absolute values of displacements along the foreseen time smaller than 5%. With $E_0 = E_{cm}$, $\eta_1 = 28 \times 10^6\ E_{cm}$·s (s = second) and $\alpha = 0.51$, this adjustment takes the creep coefficient of the rheological model to behavior such as shown in Fig. 3.

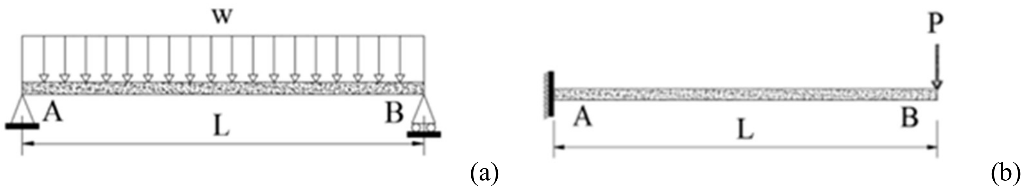

Figure 2. Beam models: (a) simply supported with a distributed loading, (b) cantilevered-free with a tip load

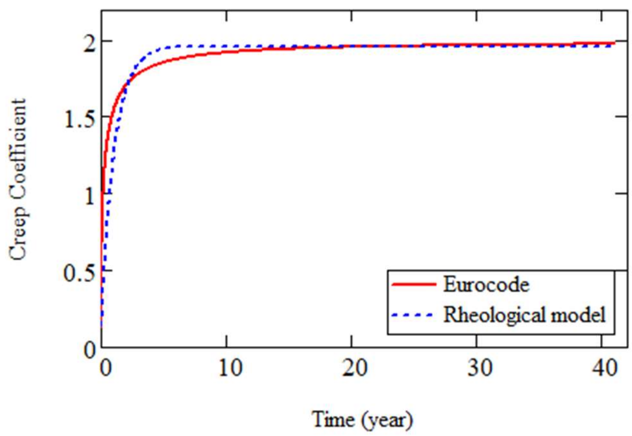

Figure 3. Creep coefficient: Eurocode, eq.(1); Rehological model, eq. (10)

4.1 Simply supported beam

A simply supported reinforced concrete beam, Fig. 2(a), is analyzed. The equation of the elastic line is as indicated in eq. (11).

$$y(x) = \frac{W}{24E(t)I}(-x^4 + 2Lx^3 - L^3x) \tag{11}$$

4.2 Cantilevered-free beam

A cantilevered-free reinforced concrete beam, Fig. 2(b), is analyzed. The equation of the elastica is as follows in eq. (12).

$$y(x) = \frac{P}{6E(t)I}(-3Lx^2 + x^3) \tag{12}$$

4.3 Material Data and Structural Arrangement Adopted

The beam geometry, assumed material properties, and calculation parameters are as follows. It is worth noting that the design of the steel reinforcement area followed the procedure specified in the European standard, without accounting for stress transfer due to concrete creep.

- Beam length: $L = 5$ m
- Cross-section dimensions, base b and height h: $b \times h = (20 \times 40)$ cm
- Uniformly distributed load: $W = 14.65$ kN/m
- Concentrated load: $P = 10$ kN
- Safety factor for forces: 1.5
- Steel safety factor: 1.15
- Cement class: N

- Concrete age at loading: 28 days
- Characteristic compressive strength of concrete: 30 MPa
- Concrete density: 2549.29 kg/m³
- Aggregate size: 19.0 mm
- Reinforcement: 4 bars of 10 mm (nominal diameter) positioned near the bottom face of the section
- Steel type: CA-50-A
- Yield strength of steel: 500 MPa
- Modulus of elasticity of reinforcement steel: 210 GPa
- Concrete cover: 3 cm
- Relative humidity of the environment: 70%
- Gravity acceleration: 9.80665 m/s²

4.4 Parallel Axis Theorem and Concrete Section Homogenization

In the present context, the homogenization of a reinforced concrete beam section represents an essential analytical procedure used in structural engineering to simplify the calculation and analysis of elements with composite cross-sections made of materials with distinct properties, such as concrete and steel in reinforced concrete. This process allows the heterogeneous cross-section of the beam to be treated as if it were composed of a single material, giving the homogenized system properties equivalent to the original system. This operation facilitates the structural analysis and prediction of behavior under imposed loads.

The homogenization process involves multiplying the areas of the steel cross-section by a homogenization factor αe, which is the ratio between the modulus of elasticity of steel (Es) and that of concrete (Ec):

$$\alpha e = \frac{Es}{Ec} \tag{13}$$

With the homogenization factor obtained, the area of the homogenized section can be calculated for the case under study. Similarly, the moment of inertia of the homogenized section can be calculated as well.

$$Ich = Ic + Ac(\Delta y)^2 + (\alpha e - 1)As(ycg - d'')^2 \tag{14}$$

where:

- Ac is the gross concrete section area,
- ycg is the y-coordinate of the centroid of the homogenized section,
- Icg is the moment of inertia of the homogenized section,
- Ic is the moment of inertia of the gross concrete section,
- Δy is the difference between the centroid of the gross section and the centroid of the homogenized section,
- d'' is the distance between the centroid of the positive reinforcement and the bottom of the beam.

This approach adjusts the steel inertia to match that of concrete, allowing the cross-section to be analyzed as if it were entirely made of a material with uniform mechanical properties. This process does not alter the overall stiffness of the beam but redistributes the properties of the constituent materials in a way that simplifies calculations.

5 Results and Discussion

For the examples defined in the numerical simulations, results were generated considering the start of concrete production 28 days before the application of the loading. Based on the formulation of the elastic line equation given by eq. (11) and eq. (12) and using the variation of the modulus of elasticity due to creep provided by eqs. (2) and (8), the total displacements of the beam at different time intervals were calculated. Figure 4 shows the elastic line of the beams for the two models obtained by numerical simulation considering the temperature of 20ºC and relative humidity of 70%, when Eurocode is used. Table 1 shows the results obtained for maximum deflections for both beam models. In Table 1 the difference is calculated considering the Eurocode as the reference.

Table 1. Maximum deflections for beam models. Result in “mm”.

t (day)	Simply supported			Cantilevered-free		
	Eurocode	Rheological model	Difference (%)	Eurocode	Rheological model	Difference (%)
28	-4.423	-4.453	-0.695	-0.385	-0.388	-0.694
90	-7.974	-5.507	30.936	-0.694	-0.479	30.936
500	-9.480	-9.480	7.321	-0.890	-0.825	7.321
1000	-10.229	-11.017	-1.718	-0.943	-0.959	-1.718
2500	-10.831	-11.592	-2.411	-0.985	-1.009	-2.411
5000	-11.319	-11.604	-0.780	-1.002	-1.010	-0.780
7500	-11.515	-11.604	-0.173	-1.008	-1.010	-0.173
10000	-11.620	-11.604	0.136	-1.011	-1.010	0.136
15000	-11.657	-11.604	0.449	-1.015	-1.010	0.449
	Average of absolute differences (%) = 4.96					

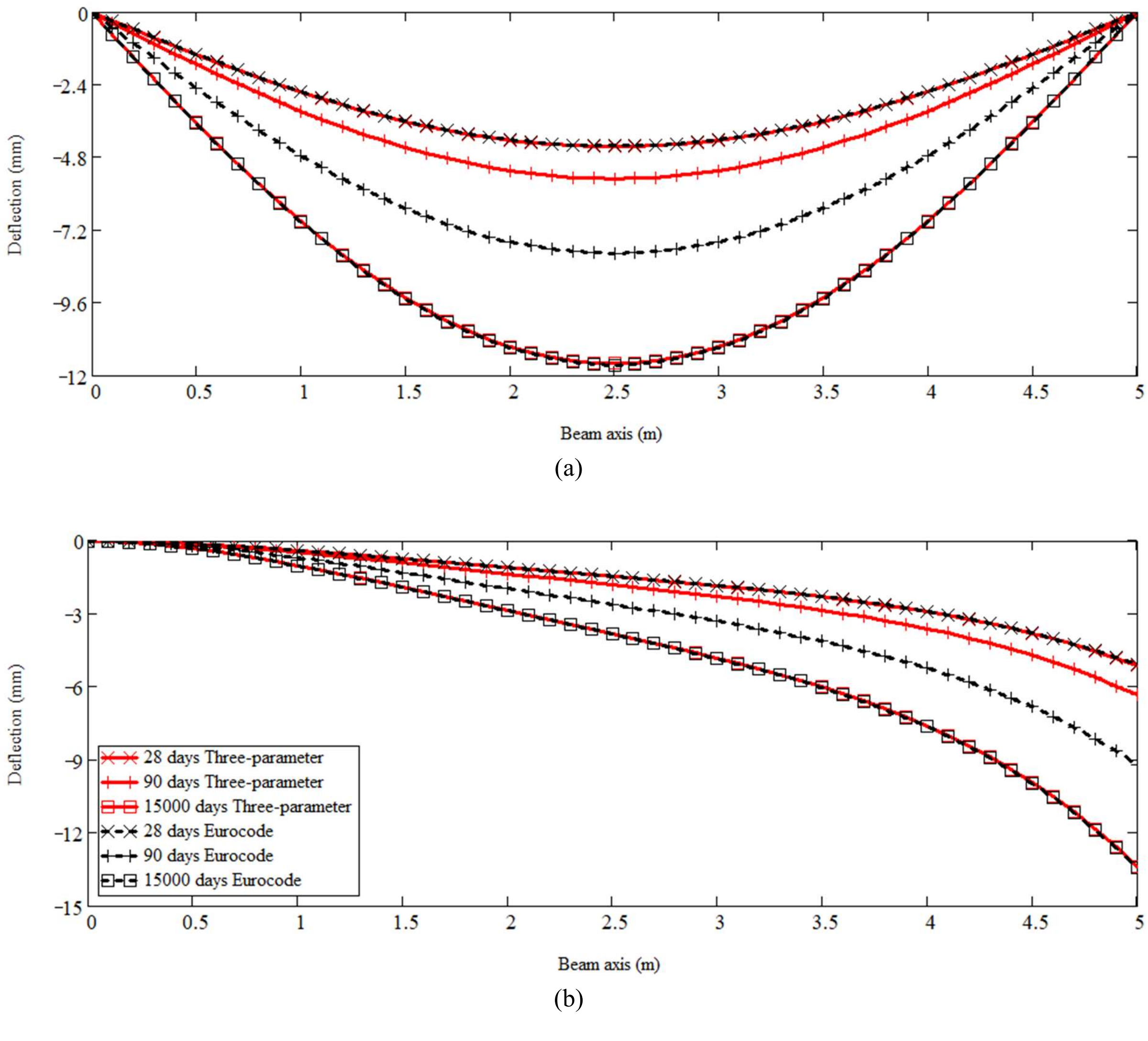

Figure 4. Deflections: (a) simply supported beam, (b) cantilevered-free beam (legend for both graphic)

6 Conclusions

An empirical definition of viscous parameters of a rheological model was performed to minimize the average difference of values obtained considering the curve of creep of Eurocode as a reference. Simulating numerically displacements of beams of reinforced concrete was possible to use the curve of a rheological model to approximate values of a code assuming an allowable error. In the present case, one smaller than 5% was adopted. Based on this concept, in this work, the rheological model of three-parameter is converted in a model only depending on the modulus of elasticity of the material and a regulator for the curve amplitude. A try and error procedure was used to define the best parameters in relation to the expected percent difference. For future works, however, a logic of programming to diminish still more the difference can be used. One potential strategy to do that is minimizing the distance between points of a curve considering another as a reference, what can be done observing a specific, judged privileged, point or all set of points generated.

Acknowledgements. To the Postgraduate Program in Civil and Environmental Engineering (PPGECEA) at the State University of Feira de Santana (UEFS) for the support provided. Also, to CNPq for the given support (process 302494/2022-7).

Authorship statement. The authors hereby confirm that they are the sole liable persons responsible for the authorship of this work, and that all material that has been herein included as part of the present paper is either the property (and authorship) of the authors, or has the permission of the owners to be included here.

References

[1] K. B. Tran, Q. S. Nguyen and T. T. Truong, "Creep Analysis of Concrete Beams and Flat-Slabs by Using Finite Element Method". Seatuc Journal of Science and Engineering, 1(1), 46-51, 2020.
[2] A. B. Giorla, "Implementation of concrete creep model in grizzly (No. ORNL/TM-2017/729)". Oak Ridge National Lab. (ORNL), Oak Ridge, TN, United States, 2017.
[3] S. Liang and Y. Wei, "Methodology of obtaining intrinsic creep property of concrete by flexural deflection test". Cement and Concrete Composites, 97, 288-299, 2019.
[4] R. Goel, R. Kumar and D. K. Paul, "Comparative study of various creep and shrinkage prediction models for concrete". Journal of materials in Civil Engineering, 19(3), 249-260, 2007.
[5] X. Shao, L. Li, and J. Yang, "Experimental research on the creep behavior and bearing capacity of repeatedly prestressed concrete beam". Frontiers of Architecture and Civil Engineering in China, 1, 305-311, 2007.
[6] E. L. Madureira, B. V. C. Fontes and J. C. N. de Araújo, "Efeitos da Temperatura nas Deformações por Fluência do Concreto". In Anais do 59º Congresso Brasileiro de Concreto. IBRACON. Bento Gonçalves, 2017.
[7] A. M. Wahrhaftig, K. M. M. Magalhães, M. A. Silva, R. M. L. R. F. Brasil and J. R.Banerjee, "Buckling and free vibration analysis of non-prismatic columns using optimized shape functions and Rayleigh method", European Journal of Mechanics - A/Solids, Volume 94, 104543, https://doi.org/10.1016/j.euromechsol.2022.104543, 2022.
[8] M. N. Hassoun, and A. Al-Manaseer, "Structural concrete: theory and design". John Wiley & Sons, 2020.
[9] M. H. Hubler, R. Wendner and Z. P. Bažant, "Statistical justification of Model B4 for drying and autogenous shrinkage of concrete and comparisons to other models". Materials and Structures, 48, 797-814, 2015.
[10] K. M. M. Magalhães, R. M. L. R. F. Brasil, A. M. Wahrhaftig, G. H. Siqueira, I. Bondarenko and L. Neduzha, "Influence of Atmospheric Humidity on the Critical Buckling Load of Reinforced Concrete Columns". International Journal of Structural Stability and Dynamics. Vol. 22, No. 01, 2250011.c. https://doi.org/10.1142/S0219455422500110, 2022.
[11] A. M. Neville and J. J. Brooks, "Concrete Technology", Pearson Educated Limited, 2nd Edition, London, 2010.
[12] K. A. Paulson, A. H. Nilson and K. C. Hover, "Long-Term Deflection of High-Strength Concrete Beams", ACI Material Journal, 88 197-206, 1991.
[13] A. M. Wahrhaftig and K. M. M. Magalhães. Effect of Creep on Stability of Structural Elements Cur Trends Civil & Struct Eng. 3(3), 2019.
[14] CEN, "Eurocode 2: Design of Concrete Structures-Part 1-1: General rules and rules for buildings, EN 1992-1-1," Brussels (Belgium), 2023.
[15] M. A. D. Carvalho, Estudo numérico-analítico de modelos reológicos unidimensionais viscoelásticos, elastoplásticos e viscoplásticos, 2014.
[16] S. P. C. Marques and G. J. Creus, Computational viscoelasticity. Springer, Heidelberg, 2012.
[17] A. M. Wahrhaftig, R. M. L. R. F. Brasil and L. S. M. S. C. Nascimento. Analytical and Mathematical Analysis of the Vibration of Structural Systems Considering Geometric Stiffness and Viscoelasticity [Internet]. Numerical Simulations in Engineering and Science. InTech. Available from: http://dx.doi.org/10.5772/intechopen.75615, 2018.